PROCEEDINGS OF SCIENCE

Fully Differential Higgs Pair Production in Association With a Vector Boson at NNLO in QCD

Chong Sheng Li
Department of Physics and State Key Laboratory of Nuclear Physics and Technology, Peking University, Beijing 100871, China
Centre for High Energy Physics, Peking University, Beijing 100871, China
E-mail: csli@pku.edu.cn

Hai Tao Li
Los Alamos National Laboratory, Theoretical Division, Los Alamos, NM 87545, USA
E-mail: haitaoli@lanl.gov

Jian Wang*
Physik Department T31, Technische Universität München, James-Franck-Straße 1, D–85748 Garching, Germany
E-mail: j.wang@tum.de

The Higgs self-coupling is an important parameter in the standard model to clarify the electroweak symmetry breaking mechanism, which can be measured via Higgs boson pair productions at hadron colliders. We present a fully differential NNLO QCD calculation of the Higgs boson pair production in association with a massive gauge boson at hadron colliders. For Whh production, the NNLO effects reduce the scale uncertainties significantly, and are sizeable in the large transverse momentum region. For Zhh production, the NNLO effects enhance the NLO total cross sections by $20\% - 50\%$, and change the shape of NLO kinematic distributions. The impact on the extraction of the self-coupling from experiments is significant. These theoretical results can be utilised in future experimental analysis.

Loops and Legs in Quantum Field Theory (LL2018)
29 April 2018 - 04 May 2018
St. Goar, Germany

*Speaker.

PoS(LL2018)021

1. Higgs self-couplings

The discovery of the Higgs boson at the LHC [1, 2] is a milestone toward understanding the mechanism of electroweak symmetry breaking. The accumulated data indicate that it is a spin-0 and *CP*-even particle with a mass of 125 GeV [3]. This mass is consistent with the constraints from the electroweak fit of the standard model. Its width has also been measured by combining the information of on-shell and off-shell Higgs productions [4], and the upper limit is around $5 \sim 7$ times the standard model predictions [5]. The couplings with heavy gauge bosons or fermions are measured to agree with the standard model expectations [6], though large uncertainties exist. So far, the data show no significant deviation from the standard model. However, this does not mean that we have known everything about this particle. The Higgs self-couplings, which are very important in understanding the electroweak symmetry breaking, have not been checked experimentally. Actually, in some new physics models, the trilinear Higgs self-coupling may change by $O(100)\%$, while the couplings with the gauge bosons and fermions are still in agreement with the standard model. Therefore, it is the task of the future LHC and other colliders to precisely measure the self-couplings.

These self-couplings can be measured through the processes of Higgs boson pair productions. There are four channels, and each of them is sensitive to the self-couplings in different ways, and thus deserves detailed studies on the same footing. There have been already a lot of papers to investigate the prospect of constraining the self-couplings at the LHC or future 100 TeV hadron colliders. Most of these studies are performed at the leading order (LO) of QCD, which suffers from large theoretical uncertainties. It is necessary to take into account higher-order corrections in order to get precise constraints. In this work, we focus on the vector boson associated production channel and present the first numerical result for the kinematic distributions at QCD NNLO [7, 8]. The sample Feynman diagrams are shown in Fig.1. Due to the accompanying vector boson, these events are relatively easier to search, compared with the gluon-gluon fusion channel, and therefore the two Higgs bosons can be searched for in the bottom quark decay channel, which has the largest decay branching ratio. As a consequence, the cross section of this channel is not much smaller than the gluon-gluon fusion channel [9]. Moreover, this channel depends on the self-coupling at tree level, thus it is more direct and clear to interpret the cross section in terms of the self-coupling.

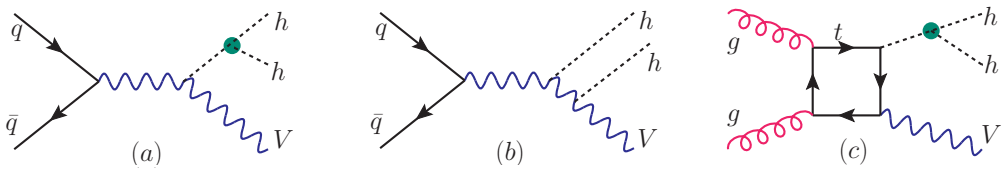

Figure 1: The sample Feynman diagrams for *Vhh* production. The diagram (c) is present only for *Zhh* production.

2. NNLO q_T subtraction based on soft-collinear effective theory

We perform the NNLO QCD differential calculations using the q_T subtraction method [10],

where q_T denotes the transverse momentum of the final-state colourless system. More specifically,

$$\frac{d\sigma_{Vhh}^{\rm NNLO}}{d\Phi_3 dy} = \int_0^{q_T^{\rm cut}} dq_T \frac{d\sigma_{Vhh}^{\rm NNLO}}{d\Phi_3 dy dq_T} + \int_{q_T^{\rm cut}}^{q_T^{\rm max}} dq_T \frac{d\sigma_{Vhhj}^{\rm NLO}}{d\Phi_3 dy dq_T} \,, \tag{2.1}$$

where $q_T^{\rm max}$ is fixed by the partonic center-of-mass energy and the phase space constraints.

The first part in the above equation can be obtained by expanding the transverse momentum resummation formula up to NNLO. We make use of the transverse momentum resummation based on soft-collinear effective theory [11, 12]. Since the process of $q\bar{q} \to Vhh$[1] can be considered as a production of an off-shell V^* boson and its decay to Vhh, the cross section of $q\bar{q} \to Vhh$ production in the small q_T region can be written as [13]

$$\begin{aligned}\frac{d\sigma_{Vhh}}{dq_T^2 dy dM^2} &= \frac{1}{2SM^2} \sum_{i,j=q,\bar{q},g} \int_{\zeta_1}^1 \frac{dz_1}{z_1} \int_{\zeta_2}^1 \frac{dz_2}{z_2} \int d\Phi_3 \\ &\times \left(f_{i/N_1}(\zeta_1/z_1,\mu) f_{j/N_2}(\zeta_2/z_2,\mu) H_{q\bar{q}}(M,\mu) C_{q\bar{q}\leftarrow ij}(z_1,z_2,q_T,M,\mu) \right) \left[1 + \mathscr{O}\left(\frac{q_T^2}{M^2}\right) \right] \,, \end{aligned} \tag{2.2}$$

where q_T, M and y are the transverse momentum, invariant mass and rapidity of the Vhh system, $d\Phi_3$ the three-body phase space, and $f_{i/N}(x,\mu)$ the standard PDF. The integration lower limits ζ_1 and ζ_2 are determined by S, M, q_T, y. The hard function $H_{q\bar{q}}(M,\mu)$ contains the contribution from hard-scale interactions and is extracted by matching the (axial) vector currents in QCD onto effective currents built out of fields in SCET. All the q_T-dependent terms are contained in the collinear kernel [13]

$$C_{q\bar{q}\leftarrow ij}(z_1,z_2,q_T,M,\mu) = \frac{1}{4\pi} \int d^2x_\perp e^{-ix_\perp \cdot q_\perp} \left(\frac{x_T^2 M^2}{b_0^2} \right)^{F_{q\bar{q}}(x_T^2,\mu)} I_{q\leftarrow i}(z_1,L_\perp,\alpha_s) I_{\bar{q}\leftarrow j}(z_2,L_\perp,\alpha_s) \tag{2.3}$$

with $x_T^2 = -x_\perp^2$, $b_0 = 2e^{-\gamma_E}$ and $L_\perp = \ln \frac{x_T^2 \mu^2}{b_0^2}$. The function $F_{q\bar{q}}(x_T^2,\mu)$ arises from the effect of collinear anomaly. The function $I_{q\leftarrow i}$ describes the evolution of a parton i to q at fixed $x_\perp$.

In the second part of Eq.(2.1), because of the constraint $q_T > q_T^{\rm cut}$, there must be at least one parton in the final state. Therefore, we need to calculate only the NLO corrections to $pp \to Vhhj$ production. The combination of phase spaces of $pp \to Vhhj$ at NLO with large q_T and $pp \to Vhh$ at NNLO with small q_T recovers the whole phase space of $pp \to Vhh$ at NNLO. In this work, we use the modified MadGraph5_aMC@NLO [14] to calculate the NLO corrections to $pp \to Vhhj$.

In the Zhh process, the cross section of the loop-induced process $gg \to Zhh$ is both ultraviolet and infrared finite, and thus there is no need to introduce a subtraction method to calculate this process. We also use MadGraph5_aMC@NLO [14, 15] to compute this contribution.

3. Numerical results

First we check that the cross section is independent of the cut-off parameter, as shown in Fig.2. We only show the case of Zhh production, and the case of Whh production is similar. It can be seen

[1]The gg channel is not included in the discussion of this part.

that the total cross section is insensitive to the choice of the cut-off parameter. As mentioned above, the prediction on $\sigma(q_T < q_T^{\rm cut})$ is only valid at leading power. The power correction is around 0.04% for $q_T^{\rm cut} = 10$ GeV and $M_{HHV} \sim 500$ GeV. Its effect on the total cross section is even smaller, since the main contribution is from $\sigma(q_T > q_T^{\rm cut})$.

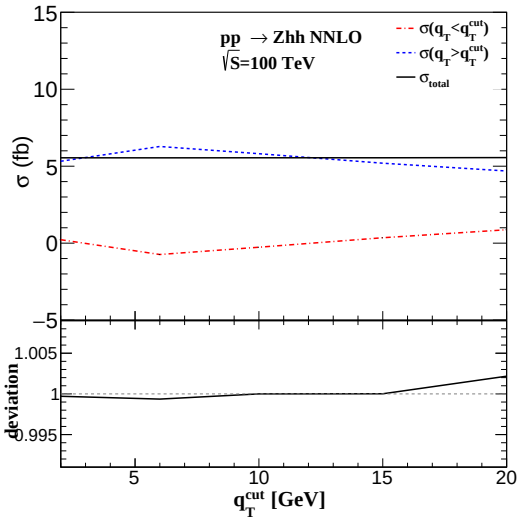

Figure 2: The total cross sections of $pp \to Zhh$ production at NNLO without the contribution from loop-induced gg fusion channel. In the bottom panels, the deviation is defined as $\sigma(q_T^{\rm cut})/\sigma(q_T^{\rm cut} = 10\ {\rm GeV})$.

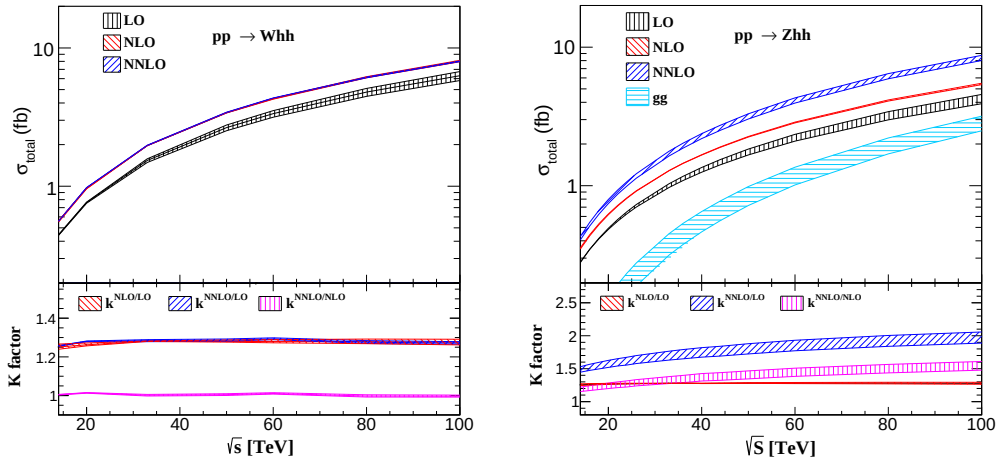

Figure 3: The total cross section of Whh (left) and Zhh (right) production as a function of the collider energy. The bands denote the scale uncertainties when varying $\mu = \mu_F = \mu_R$ by a factor of two. The NNLO total cross sections of Zhh production also include the loop-induced gg channel, and the contribution from this channel is also shown in the upper panel individually.

Then we present the result for the total cross section at hadron colliders with different energies in Fig.3. We observe that the NLO corrections are around $25\% - 30\%$ for both Whh and Zhh production. The NNLO correction for Whh production is very small while that for Zhh production

is significant, increasing the NLO result further by $20\% - 50\%$. The reason is the contribution of the new gg channel, which is shown in the diagram (c) of Fig.1, at NNLO in Zhh production. This new channel is of order α_s^2, but gets enhanced by the large gluon luminosity. As a result, its contribution is significant, about $13\% - 34\%$ of the total NNLO result. The scale uncertainties are reduced at NLO and NNLO for Whh production. For Zhh production, the scale uncertainties are reduced at NLO, but increased at NNLO due to the contribution from the new gg channel. It is expected that higher-order effects in this new channel can reduce these uncertainties, which requires the calculation of two-loop virtual diagrams with several mass scales. We leave it to future work. By adopting the same input parameters, our calculations of the total cross sections are consistent with those in Ref.[16].

The predictions on the kinematic distributions are shown in Fig.4. We can see that the NLO and NNLO effects are more significant in the large transverse momentum region for the Whh production. In contrast, the NNLO corrections for the Zhh production are most important in the peak region, where the cross section is increased by 80% from NLO to NNLO. Moreover, the shape of the distribution also changes, which means that one can not use a universal K-factor to estimate the higher-order corrections in this process.

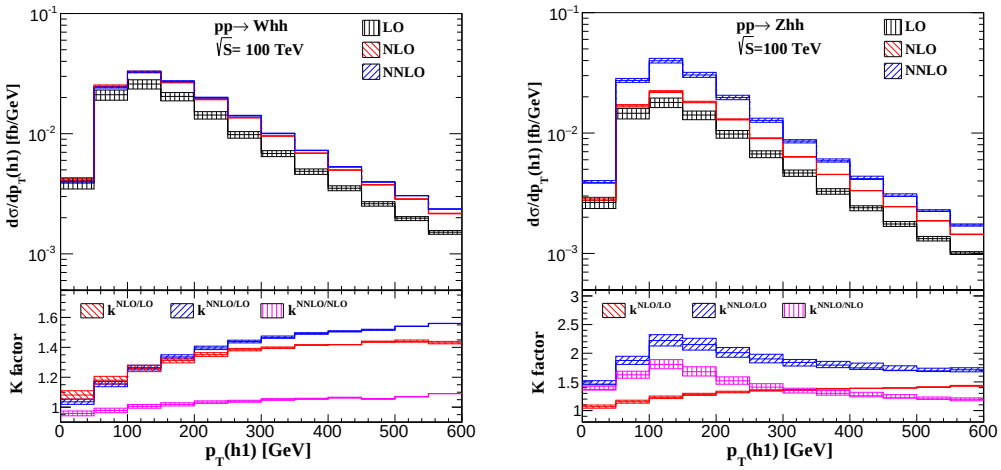

Figure 4: The transverse momentum distributions of the leading Higgs boson in Whh (left) and Zhh (right) production.

Lastly, we show the dependence of the cross section on the self-coupling in Fig.5. We see that the cross sections are sensitive to the self-coupling, especially if it is positive. For Whh production, the NLO and NNLO results are almost the same for different values of the self-coupling. For Zhh production, the NNLO correction changes the dependence on the self-coupling significantly. For example, if the measured cross section of Zhh production is about 8 fb, then the extracted self-coupling is about 2.6, 2.0 and 1 at LO, NLO and NNLO, respectively, where we have assumed that the self-coupling is positive. Actually, since the dependencies are shown in quadratic curves, there are generally two values of the self-coupling corresponding to the same cross section. In order to break this degeneracy, it is desirable to make use of the kinematic distributions [7, 8] or to combine the information of the other Higgs boson pair production channels.

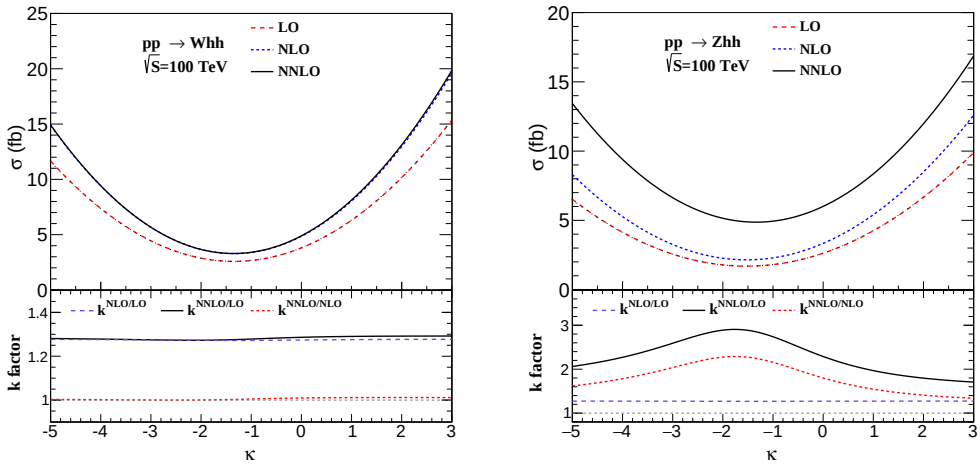

Figure 5: The dependence of the cross section on the self-coupling in Whh (left) and Zhh (right) production. The parameter κ is defined by $\lambda_{hhh} = \kappa\lambda_{hhh}^{\mathrm{SM}}$.

4. Acknowledgements

CSL was supported partly by the National Nature Science Foundation of China, under Grants No. 11375013. HTL was supported by the U.S. Department of Energy Early Career Program. JW was supported by the BMBF project No. 05H15W0CAA.

References

[1] ATLAS Collaboration, G. Aad *et al.*, Phys.Lett. **B716**, 1 (2012).

[2] CMS Collaboration, S. Chatrchyan *et al.*, Phys.Lett. **B716**, 30 (2012).

[3] CMS, V. Khachatryan *et al.*, Phys. Rev. **D92**, 012004 (2015).

[4] F. Caola and K. Melnikov, Phys. Rev. D **88**, 054024 (2013).

[5] V. Khachatryan *et al.* [CMS Collaboration], Phys. Lett. B **736** (2014) 64

[6] ATLAS, G. Aad *et al.*, Phys. Lett. **B726**, 88 (2013), 1307.1427, [Erratum: Phys. Lett.B734,406(2014)].

[7] H. T. Li and J. Wang, Phys. Lett. B **765** (2017) 265.

[8] H. T. Li, C. S. Li and J. Wang, Phys. Rev. D **97** (2018) no.7, 074026.

[9] Q.-H. Cao, Y. Liu, and B. Yan, Phys. Rev. **D95**, 073006 (2017).

[10] S. Catani and M. Grazzini, Phys. Rev. Lett. **98**, 222002 (2007).

[11] C. W. Bauer, S. Fleming, D. Pirjol, and I. W. Stewart, Phys.Rev. **D63**, 114020 (2001).

[12] C. W. Bauer, D. Pirjol, and I. W. Stewart, Phys.Rev. **D65**, 054022 (2002).

[13] T. Becher and M. Neubert, Eur. Phys. J. **C71**, 1665 (2011).

[14] J. Alwall *et al.*, JHEP **07**, 079 (2014).

[15] V. Hirschi and O. Mattelaer, JHEP **10**, 146 (2015).

[16] J. Baglio *et al.*, JHEP **04**, 151 (2013).